LEVEL 4 (1)

SEPARATION CONTROL IN THE
ALL APT LIGHT PIPE.

THESIS

AFIT/GAE/AE/79D-1

Wade H. Bailey, Jr.
Captain   USAF

AFIT/GAE/AE/79D-1

SEPARATION CONTROL IN THE

ALL APT LIGHT PIPE

THESIS

Presented to the Faculty of the School of Engineering

of the Air Force Institute of Technology

Air University

In Partial Fulfillment of the

Requirements for the Degree of

Master of Science

by

Wade H. Bailey, Jr.
Capt   USAF

Graduate Engineering

December 1979

Acknowledgments

Contents

List of Figures

List of Symbols

A = area, ft^2

a = local speed of sound, ft/sec

c_p = specific heat, b/lb_m-F

d = pipe diameter, ft

g = acceleration due to gravity, 32.2 ft/sec^2

I = energy absorbed by the gas, b/sec-ft^2

I_A = energy absorbed by the gas per unit length, B/sec-ft^3

I_o = initial energy of the beam, B/sec-ft^2

k = monochromatic absorption coefficient / ft

L = characteristic length of absorption, ft

M = Mach number, non-dimensional

$\dot{m}$ = mass flow rate, 1bm/sec

n = index of refraction, non-dimensional

p = gas pressure, $1b_f/ft^2$

R = Universal Gas Constant, 53.54 ft-$1b_f/1b_m$-R

R_e = Reynolds number, non-dimensional

T = temperature, R or F

t = time, sec

V = freestream velocity, ft/sec

β = Gladstone-Dale constant, .1134 $ft^3/1bm$

Δ = a difference

δ = phase angle difference, wavelengths

Γ = optical path difference (OPD), ft

λ = laser wavelength, ft or μm

ν = kinematic viscosity, ft^2/sec

ρ = gas density, lbm/ft^2

Subscripts

$(\ )_d$ = based on pipe diameter

$(\ )_o$ = total or stagnation value

$(\ )_x$ = air of certain index of refraction

Abstract

An experiment was performed to determine separation regions inside a high energy laser (HEL) beam relay light pipe. The pipe is part of the beam relay system used in conjunction with the CO_2 Gas Dynamic Laser (GDL) system under development by the Air Force Weapons Laboratory. It was found that the air flowing through the pipe separated at the elbows. This separation can cause uneven radial heating attributed to molecular absorption. The self-induced thermal distortion of the beam can cause phase distortions degrading the beam. A study of separation control systems within the pipe was made.

A full-scale axisymmetric model was studied on the water table. Areas of separation were found by flow visualization using dye injection. A brief evaluation of suction and blowing to control separation showed both of these methods acceptable. Separated regions discovered at each elbow on the water table were the focus of study for a full-scale air flow plexiglass model. The turbulent flow in the pipe was studied using smoke injection to reveal air motion in the pipe. Mass flow rates of air through the pipe were 1 lb/min and 8 lbs/min. Suction and blowing were assessed as flow separation control methods.

Blowing high speed air downstream of the inside of

each elbow proved unacceptable as the outside of the pipe experienced flow reversal. Suction downstream of each elbow using small slots removed the separated regions completely at $\dot{m} = 1$ lb/min. Calculations of absorption within each of the separation regions for the flow rates of 1 and 8 lbs/min were made. Absorption calculations showed further that the 1 lb/min flow had temperature rises of   F and an associated phase distortion of 3 waves at 10.6 μm. The 8 lbs/min flow rate experienced a 2 F temperature rise, yielding a distortion of 0.1 wave at 10.6 μm.

It is recommended that suction as a means of separation control be applied to low mass flow rates through the tube due to unacceptable distortions to the beam. At high mass flow rates through the pipe, suction may not be possible; however, the associated beam distortions may be acceptable.

SEPARATION CONTROL IN THE

ALL APT LIGHT PIPE

I. Introduction

Background

The Air Force is currently developing an airborne
high energy laser (HEL) weapon system. Research is being
conducted at the Air Force Weapons Laboratory (AFWL) utilizing
a modified KC-135, referred to as the Airborne Laser Labora-
tory (ALL). A CO_2 Gas Dynamic Laser (GDL) is the device
undergoing testing for installation on the ALL. The CO_2
laser emits radiation at a wavelength of 10.6 micrometers,
which is in the near-infrared. The laser beam is generated
within the aircraft fuselage and requires a long beam path
composed of mirrors and optical sensors to be transmitted
to the laser turret mounted atop the aircraft fuselage. This
beam path is known as the optical train. The laser beam is
exposed to various degrading phenomena while transiting the
optical beam path. Among these are molecular absorption. If
any of these degrading influences become severe enough, then
the power per unit area delivered to a target will be dimin-
ished because the ability to obtain focus in the far-field
may be lost. Thus, the overall effectiveness of the laser
weapon is reduced.

Problem

The laser system associated with the ALL employs a complicated optical train from the GDL to the turret atop the aircraft. The last stage of the path uses a pipe equipped with mirrors to route the laser beam from the bottom of a rotatable turret to a point in the side of the turret where an expanding telescope is housed. The "light pipe" is part of the ALL Airborne Pointing and Tracking (APT) system which permits the laser beam to lock onto and radiate a target. Figure 1 shows the light pipe location in the optical train. Provided that the air within the optical train is relatively dust-free, then a major cause for laser beam degradation for the CO_2 laser is molecular absorption, i.e., heating of the air by the CO_2 radiation. Heating the air causes a change in the index of refraction. To prevent uneven heating across the beam diameter, air is pumped through the optical train to promote thermal mixing. A potential problem arises when the air is pumped through the APT light pipe.

As the air is pumped through the light pipe, the mirror equipped right angles that turn the beam will cause the air to form a separated region downstream of each turn. These "dead" areas of air in the light pipe have become separated from the mixing influence of the main flow. The dead regions heat up through molecular absorption and cause hot spots in the pipe, i.e., a radial temperature gradient across the pipe. If the associated refractive index change across the pipe is great enough, the laser will suffer phase distortions affecting

2

EXPANDING
TELESCOPE

LIGHT
PIPE

MIRRORS

GAS
DYNAMIC
LASER

TURRET

LASER
BEAM

AIRCRAFT
FUSELAGE
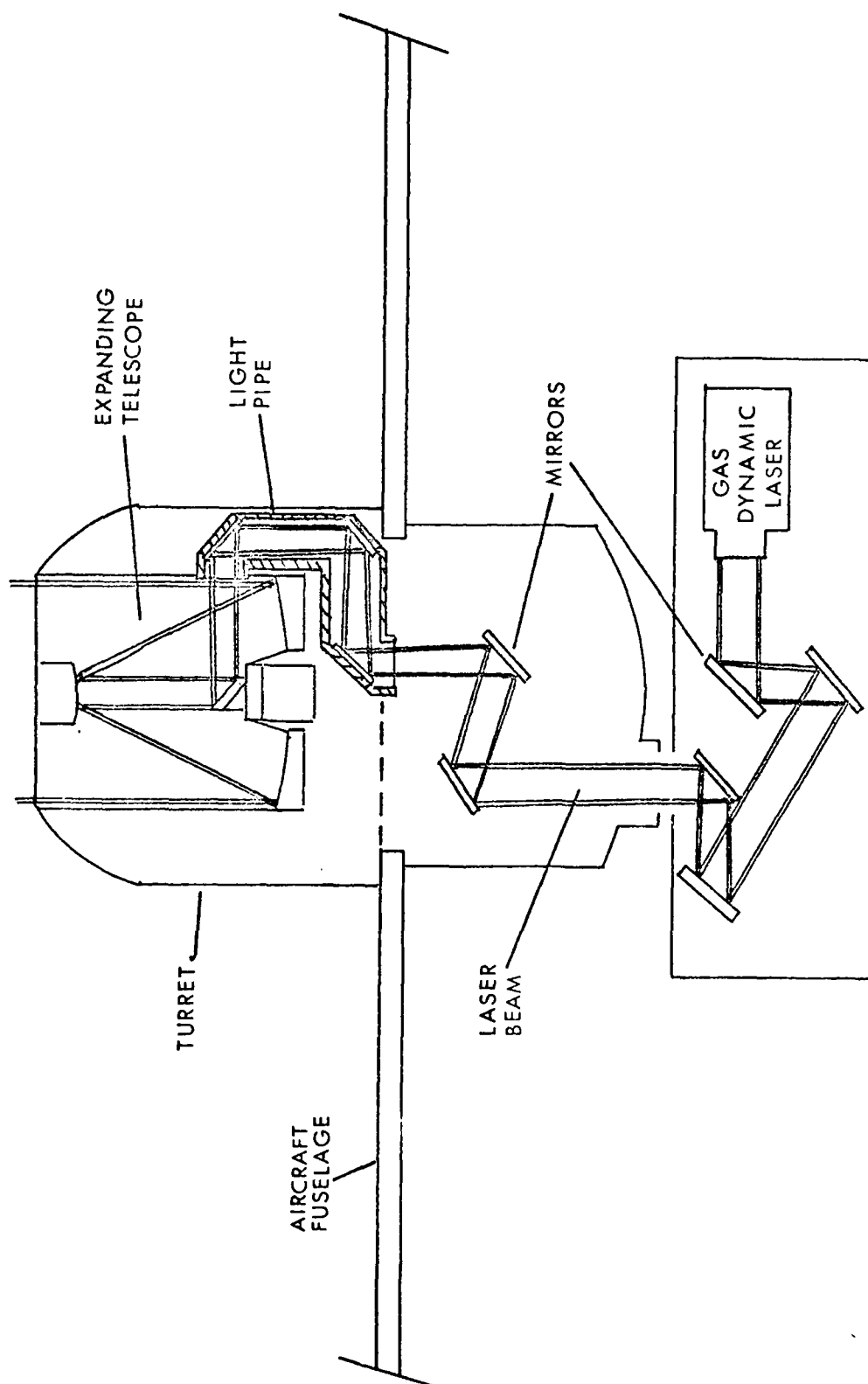
Fig 1. ALL HEL Schematic

3

its overall performance.

The focus of this research effort is to determine the extent to which the separated regions would degrade the laser beam. Also, if degradation is severe enough, analyze and recommend a separation control system capable of reducing the separation regions for minimal degradation. Associated with any research effort are constraints, and this effort is not any different.

The approach to this effort is bounded by several constraints. The foremost of these is that the light pipe is an existing piece of hardware, in place on the ALL APT, and being used in daily testing. Its placement in the ALL turret is such that there is limited clearance around the pipe. The clearance is such that a rounding of the corners is not possible. Also, any modifications for separation control will have to fit in the existing spaces. The internal diameter of the light pipe is completely filled by the laser beam which dictates that any separation control device will have to be mounted flush with the wall of the pipe. The final consideration is that the air flowing through the optical train is restricted to the mass flow rates of 1 to 8 lbs/min. The light pipe cannot be sealed with windows and evacuated because windows do not exist that could withstand the high energy beam.

Approach to Problem

Based on the pipe flow rates of 1 and 8 lb/min and the light pipe diameter of 5.25 inches, Reynolds numbers based on

4

the pipe diameter can be calculated from

$$Re_d = \frac{Vd}{\nu} \qquad (1)$$

The range of Reynolds numbers is 36,500 to 2800 for the 8 and
1 lb/min mass flow rates respectively. Because of the sharp
inlet, the turns in the pipe, and the range of Reynolds numbers,
the flow in the pipe can be expected to be turbulent (Ref 1:432).
Analytical solutions to curved pipe flows require assumptions
that could render the details of the flow separation and re-
attachment around the 90 degree turns unattainable (Ref 2:122).
Knowledge of 1) the dimensions of the separated regions and
2) the time interval it takes to completely replenish the
separation region's entrapped fluid mass by the freestream
fluid (the turnover time) is required to calculate the extent
of degradation due to molecular absorption. Simplified analy-
tical considerations would not yield these sizes and times.
For these reasons, an experimental approach was chosen, the
results of which would be applied to molecular absorption
theory.

The experimental approach consisted of two phases. The
first was a full-scale half pipe model used on a water table.
The second was a full-scale plexiglass model with flowing air.
The water table would allow the complete flow field within
the pipe to be scanned. A feel for the extent of separation
could be obtained from this scan. The air flow model could
then be used to conduct a detailed study of the separated
regions and their sizes and turnover times. At this time,

Lockheed Missiles and Space Co., Inc. is investing time and money into a water table study of a more complicated optical light pipe for a second generation APT system. The second phase of this experiment can serve to indicate the validity of the sole use of a water table for the study of light pipes.

Both phases of the experiment were utilized to test methods of reducing regions of separation. The methods considered for separation control that best met the constraints were the following: 1) suction, 2) blowing, and 3) inlet modification.

The first consideration to look at is the treatment of molecular absorption and its application to the experimental results, followed by the fluid parameters which will be studied in the water table and gas flow experiment. A detailed description of experimental phases will be next, with an in-depth analysis of the results. Drawing on the experimental results, an overall discussion of the results as applied to absorption theory will follow. Finally, conclusions will be drawn and recommendations made. With the problem and approach in mind, attention is directed to the implications of molecular absorption.

II. Analysis of Molecular Absorption

The Absorption Phenomenon

The phenomenon of molecular absorption in gases occurs when electromagnetic radiation is absorbed by gas molecules. The energy absorbed by the gas caused the outer electrons of the atoms to change energy levels. When these electrons step down to their original state, heat is emitted and the gas rises in temperature. As the temperature of the gas rises, the index of refraction changes. Absorption plays an important role daily as harmful near-infrared bands of solar radiation are absorbed by water vapor high in the atmosphere (Ref 3:11). Absorption has been researched extensively by the meteorological community (Ref 4:364) and in furnace operations as related by Hottel (Ref 5:82).

Absorption plays a detrimental role in the transmission of CO_2 laser radiation, which is in the near-infrared with a wavelength of 10.6 micrometers. Naturally occurring water vapor and carbon dioxide in air are strong absorbers of CO_2 laser radiation. Considerable research has been conducted by McClatchey in the transmission of 10.6 micrometer radiation through the atmosphere (Ref 6). The degrading effect that absorption has on laser transmission is not so much in the loss of power, but in the bending and scattering of the laser rays due to refractive index changes. The complete

7

process of laser radiation being absorbed by a gas, the gas heating up, and the light rays being distorted by the refractive index change is termed "thermal blooming." The self-induced thermal distortion of thermal blooming is covered at length by Smith (Ref 7).

The air that is flowing through the light pipe will heat up due to molecular absorption. Were no separation to occur within the pipe, the high-power laser beam would encounter a uniform index of refraction across the beam diameter due to the turbulent mixing. The beam would suffer minimal distortion due to uniform absorption. In the light pipe under consideration, a tenth wavelength distortion due to absorption at 10.6 μm would occur (Ref 8:2729). The tenth wavelength is the phase difference between the center of the beam to the edge of the beam. The light pipe does, however, have separated regions giving rise to non-uniform absorption. The uneven absorption radially across the beam due to separation would cause the beam to experience a refractive index gradient across the beam diameter which may be extensive enough to exceed the acceptable tenth wave distortion. Figure 2 illustrates the effects of uniform versus non-uniform absorption. The uniform absorption acts like a large uniform lens bending the light rays uniformly. There is some loss of power, but the far field beam is capable of being focused in a desired plane. On the other hand, large phase distortions of the beam associated with non-uniform absorption causes some loss of power but, more importantly, may defocus the beam in the

8

DENSITY
GRADIENT

LASER
BEAM

LOSS OF POWER
UNIFORM BEAM

A. Uniform absorption

DENSITY
GRADIENT

LASER
BEAM

LOSS OF POWER
DEFOCUSED
NON-UNIFORM BEAM
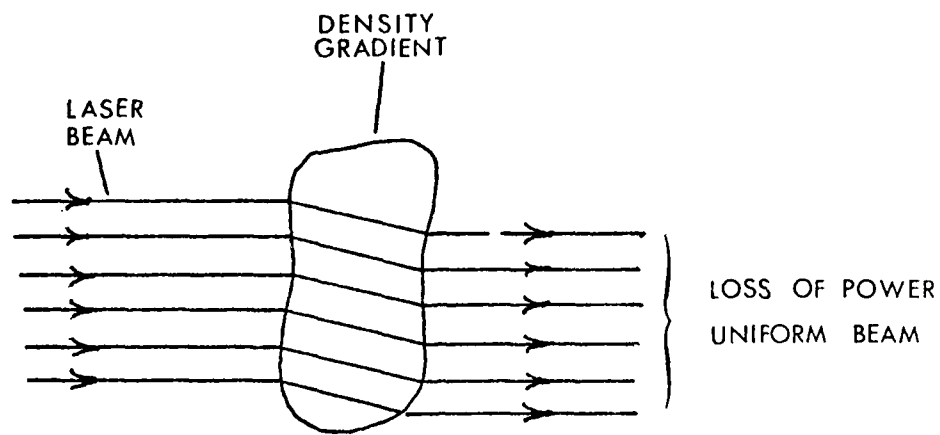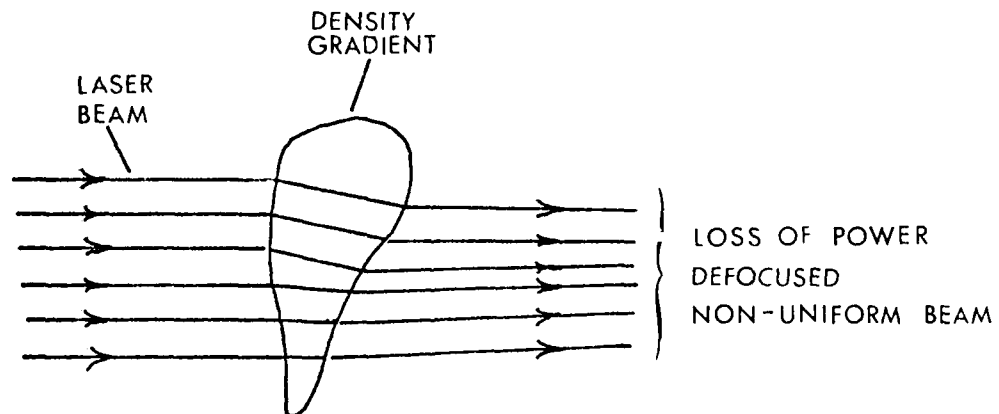
B. Non-uniform absorption

Fig 2. Effect on Uniform Laser Beam By
Density Gradient Formed by
Absorption

9

far field to a point where the existing optics cannot compensate to refocus.

The considerations for the light pipe will assume that only the separated regions experience absorption. Obviously, the freestream is being heated, but it is this heated air that is supplying air to the separated regions. The separated region will heat up even beyond the freestream temperature so that the change in the index of refraction can be considered rather than considering an absolute index change. Attention can now be turned toward the theoretical considerations of molecular absorption.

Theory

Determination of the effect of absorption begins with the basic equation (Ref 9:236):

$$I = I_o (1 - e^{-kL}) \qquad (2)$$

Since the absorbed power in the light pipe is considered negligible, the total power along the beam path can be assumed constant and the absorbed radiation can be represented by (Ref 8:2729):

$$I_A = I_o k \qquad (3)$$

Since temperature is an intensive property of the gas, the characteristic length can be omitted and the temperature rise for a characteristic volume associated with the separated region can be found from

10

$$\Delta T = \frac{I_A}{\rho C_p} \Delta t \qquad (4)$$

From the density change associated with the increase in temperature, a change in the refractive index can be calculated. The associated density change can be found from the equation of state for a perfect gas

$$\rho = \frac{P}{RT} \qquad (5)$$

Once the density of the separated region's heated gas is known, the refractive index can be found from the Gladstone-Dale law (Ref 10:21)

$$n = 1 + \beta\rho \qquad (6)$$

Finally, a measure of the amount of influence the temperature rise had on the beam can be made by calculating the optical path difference (OPD). By comparing path lengths on opposite sides of the light pipe where one light ray encounters separation and the opposite light ray is free from changes in the index of refraction, an OPD can be produced. The equation for the OPD is (Ref 10:169):

$$\Gamma = L_2 n_2 - L_1 n_1 \qquad (7)$$

The phase distortion of the beam, using the calculated OPD, is given by (Ref 10:169):

$$\delta = \frac{2\pi\Gamma}{\lambda} \qquad (8)$$

11

In order to apply these equations, the experimental measure-
ments required must be specified and the associated separation
control systems laid out. This will be covered in the follow-
ing section: the experiment.

III. The Experiment

Requirements

The experimental approach to the problem consists of two phases: 1) a qualitative inspection of the pipe flow characteristics with an initial evaluation of possible separation control systems; and 2) a full-scale study of the separated regions and implementation of the flow separation control systems.

In order to evaluate the fluid flow characteristics in the pipe, the first phase of the experiment will employ the use of a water table. The water table, relying on hydraulic analogy, provides the experimenter with a means by which an understanding of the flow field character can be had by strategically placed dye.

The second phase will use a full-scale mock-up of the ALL APT light pipe, constructed of plexiglass to allow smoke studies to be performed. This model will use air, simulating as closely as possible the real light pipe conditions while evaluating the separation control methods scanned in phase one. Both models will have the dimensions of the operational light pipe as shown in Fig 3. It is in this phase of experimentation that separation region sizes and turnover times can be measured. Also, it can be seen how closely the water table represented the gas flow model.
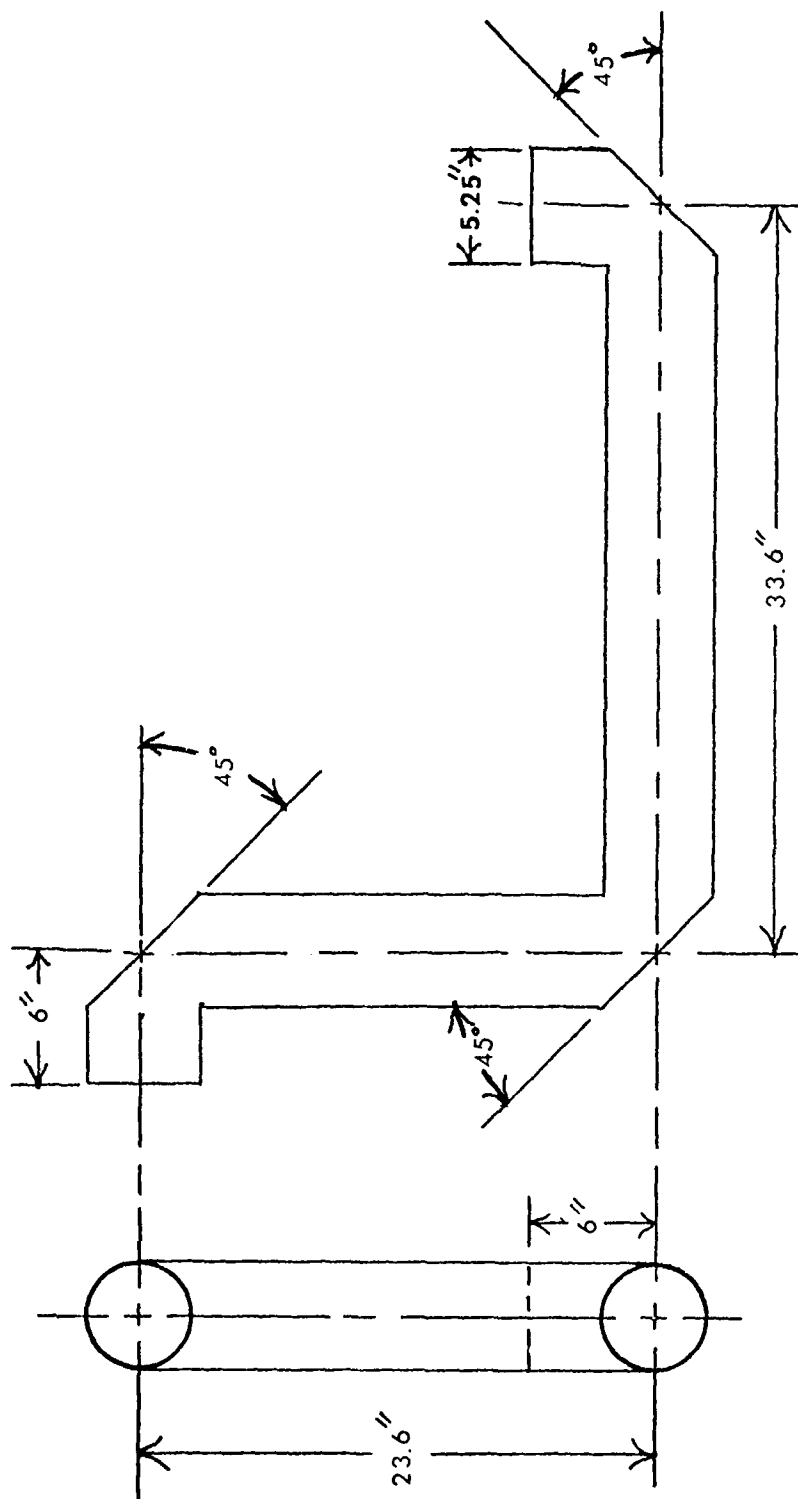
Fig 3. Dimensions of ALL APT Light Pipe As Installed

14

In this experiment, the air flowing through the light pipe had to be dynamically reproduced on the water table to conduct phase one. Appendix A gives the development of the hydraulic analogy to determine the parameters that had to be matched between the air flow and the water flow. It was found that by matching Reynolds numbers between the two flows, the water table would simulate the air flow in the pipe. The following air to water flow velocities were found:

Air	Water
1 ft/sec (1 lb/min)	0.1 ft/sec
13 ft/sec (8 lb/min)	1.0 ft/sec

For the accuracies involved in measuring velocities in water, the corresponding velocities were rounded to the nearest tenth.

The separation control systems to be evaluated were restricted to suction, blowing, and inlet modification. Both suction and blowing were implemented immediately downstream of the first two turns in the pipe for the gas flow model, but downstream of the second turn only for the water table model since the water table was a test-bed for the gas flow model. Phase I will now be reviewed in detail.

Phase I: Water Table Study

Apparatus. The water table used was a Bowles Engineering Corporation 4 ft by 6 ft, dual reservoir, No. 0535, with a maximum flow rate of 25 gpm. Flow visualization was accomplished by using dye injection. The dye was a solution of water and potassium permanganate, which was deep purple in

15

color. The dye injection was recorded with a Crown Graphic camera by Grafiex, Inc. Polaroid Land roll film, black and white, 3000 speed, Type 47 was used in the camera.

The water table experimental configuration is shown in Fig 4. The model was a full-scale, axisymmetric (duct) constructed of fiberglass. The model was painted white to provide contrast for the dye injection.

Procedure. The water table experiment was conducted in two parts. The first part consisted of a scan of the entire flow field in the pipe to determine the overall flow characteristics. The scan consisted of the two representative velocities only, i.e., 1 ft/sec and 0.1 ft/sec. Of the many types of velocity measurements that could be made, velocity of a dye droplet between two points was chosen because of the turbulent nature of the flow. By inserting a drop of dye into a straight section of the duct and timing the mid-point of the dispersed dye as it traveled through the distance of one foot, the velocity of the flow was estimated.

Flow visualization was the technique employed to study the flow. Dye was injected with a hypodermic needle below the surface of the water and a photograph was taken as the dye conformed to the flow field. This procedure was used throughout the water table study. Photographs of dye injection for the complete study are contained in Appendix B and will be discussed in detail in the results section.

Results. The dye injection allowed the entire flow field to be "mapped" before attempting any separation control.

DAM

FLOW

WATER LEVEL

SYRINGE

WEIR

CAMERA

LIGHT PIPE MODEL

PUMP

FLOW

RESERVOIRS
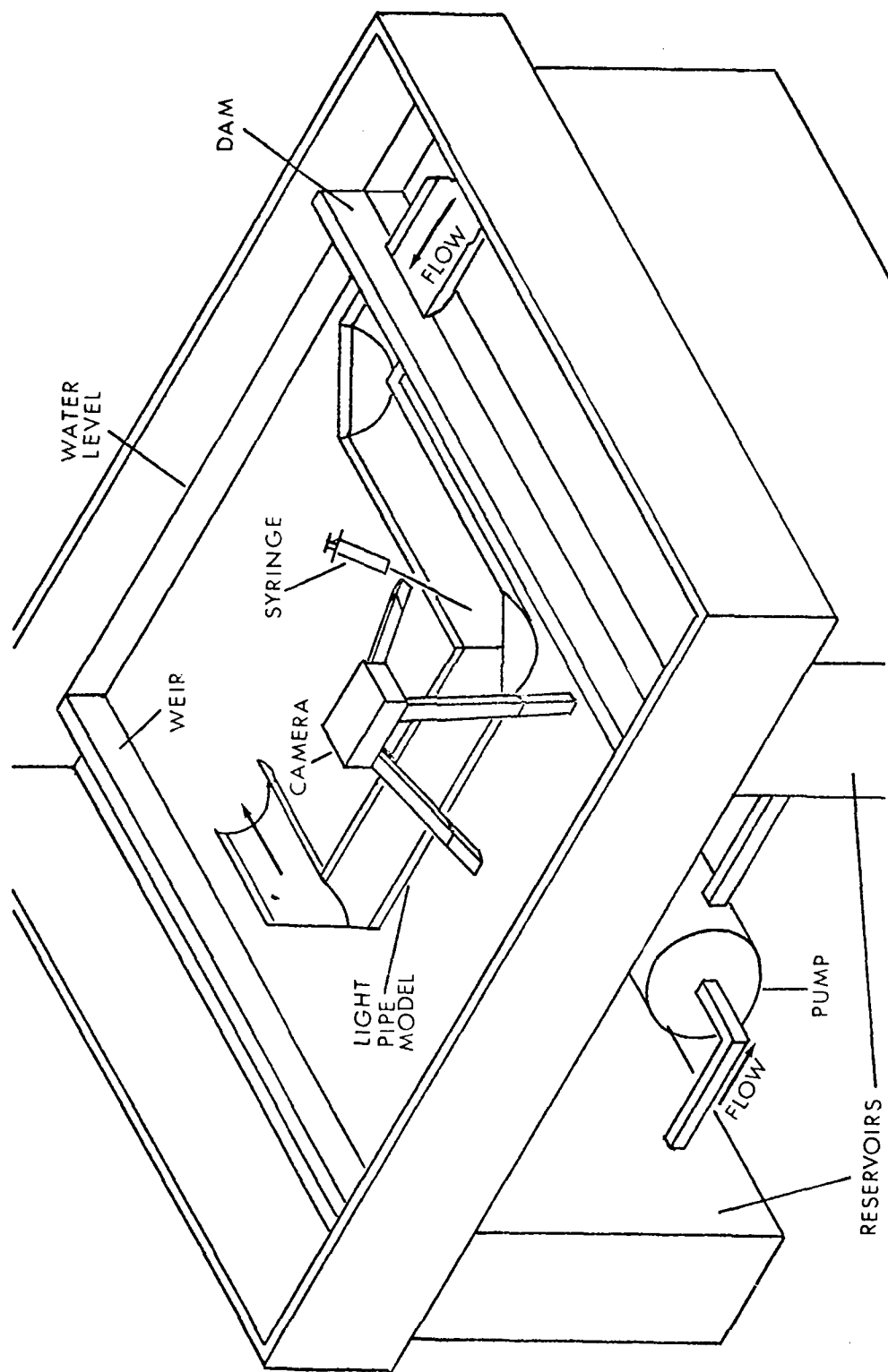
Fig 4. Water Table Experimental Set-Up

Figures B-1 through B-3 show the inlet flow patterns for a velocity of 1 ft/sec. A separation region was revealed just inside the inlet as seen in Fig B-1C. Figures B-1 and B-2 highlight the entrance streamlines as they skirt a separation region. The turbulent nature of the flow is shown by the widening and dissipation of the injected dye. Figure B-3 shows the extent of separation as dye is injected in and around the inlet corner. The extent of inlet separation can be seen to decrease slightly with the velocity of 0.1 ft/sec in Fig B-4. The turbulence of the fluid is evident by the trail of dye. The channel between the inlet and the second turn is also seen to be turbulent (Fig B-5). Figures B-6 and B-7 show that there is a large separated region associated with turn #2 at V = 1 ft/sec. Turn #2 at V = 0.1 ft/sec was photographed by injecting a large amount of dye upstream of the turn, withdrawing the syringe, and allowing it to follow the flow. Figure B-8 shows the separated region darken as it entraps the passing dye. The exit had no associated separation as seen in Fig B-9.

After a close scan of the flow in the pipe, three major areas of recirculation were found which could lead to uneven radial heating due to absorption. The three areas are shaded in Fig 5. These areas are as follows: 1) just inside the inlet; 2) after the first 90 deg turn; and 3) after the second 90 deg turn. In order to alleviate these recirculation zones, three methods of separation control were tried on the water table to evaluate the applications to be applied in phase two

18

of the experiment where any adverse flow effects could be studied.

In order to remove the separation bubble at the inlet turn, the inlet geometry was modified into a bell mouth with a radius of the inlet the same as the radius of the pipe. This modification is within the physical constraints of the problem. Figure 6 shows the inlet modification. Figures B-10, -11, and -12 show the effect the inlet modification had on the flow pattern. For both flow velocities, the separation just inside the inlet was suppressed. The extent of separation associated with the corners remain the same. The flow was laminar to the first turn and there its turbulent nature returned. After the first turn in the pipe, the inlet modification seemed to have little effect to the flow field downstream as illustrated by Fig B-13.

The next method of separation control was suction, which employed an array of 1/16 inch holes placed just downstream of the second turn. A manifold was fixed to the back of the water table model behind the holes to remove the water with a pump. The schematic of the suction system is shown in Fig 8. Suction was provided by a Shop-Vac. The amount of suction was varied by regulating the water/air suction ratio manually. Figure B-14 shows that the available suction provided by the Shop-Vac had an influence on separation at 1 ft/sec, but did not remove the area completely. The flow of $V = 0.1$ ft/sec showed favorable results with suction by reducing the separation considerably as seen by a comparison

19

PATH 'A'

TURN #1

FLOW →

PATH 'B'

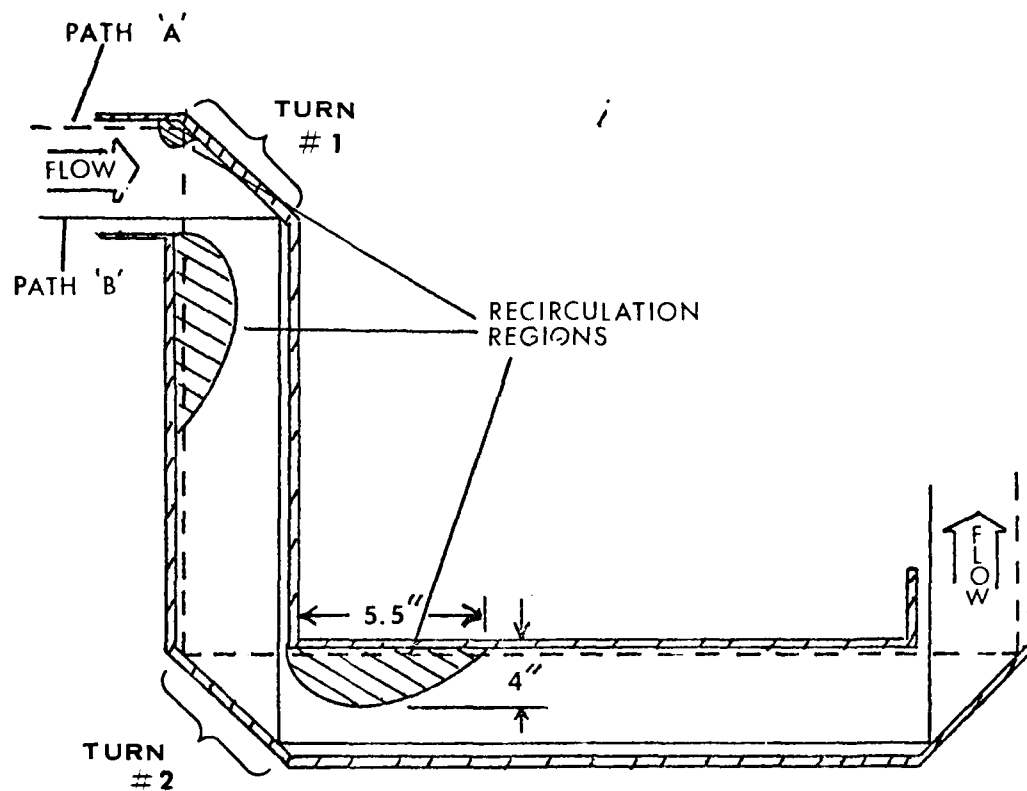RECIRCULATION REGIONS

5.5"

4"

FLOW

TURN #2

Fig 5.   Light Pipe Model With Areas
of Fluid Separation

R = 2.12"

FLOW →
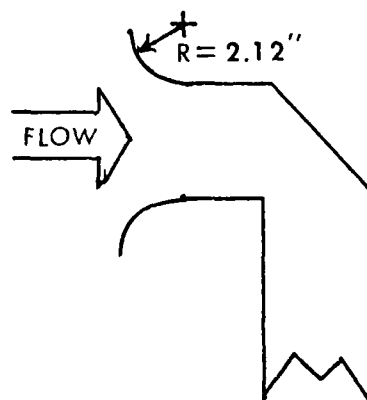
Fig 6.   Inlet Modification for Water Table Model.
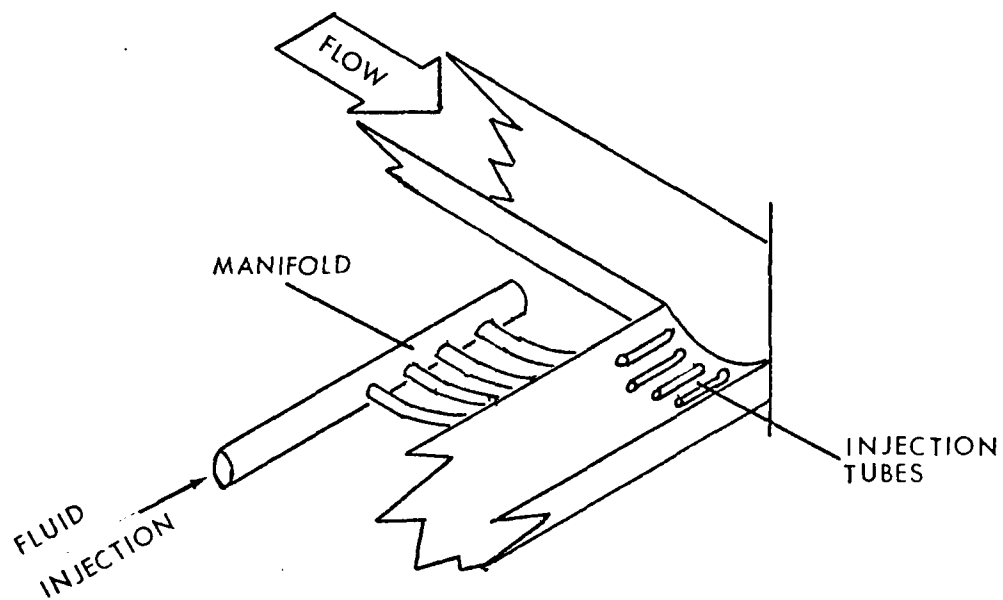
Fig 7. Mass Injection Modification for
Turn #2 on Water Table Model
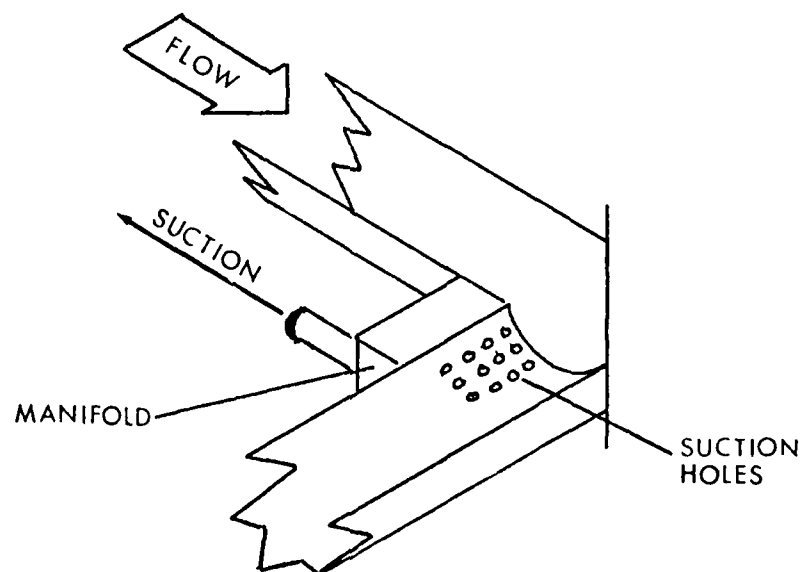
Fig 8. Suction Modification for
Turn #2 on Water Table Model

of Figs B-15A, -15C and Figs B-15B, -15D. The suction used was 7 lb/min.

Mass injection or blowing was the next separation control method studied. Four holes were drilled immediately downstream of the second turn. Three-eights inch tubing was inserted into these holes to provide the blowing. Water for blowing was provided via a water faucet. Figure 7 is a schematic of the mass injection system used. Relative to the free-stream, the tubes were varied in their injection angle: 1) normal; 2) 45 deg inclination downstream; and 3) tangential. In each case, the injection rate was varied until the separation region was minimized. The mass flow injection rates were determined by injecting into a container of known volume and timing the event. Injection was accomplished at freestream velocities in the model of the 0.1 fps to 1.0 fps. Figure B-16 shows injection normal to the flow with no reduction of separation. Figures B-17 and B-18 show blowing at 45 deg directly downstream. Both velocities experienced a reduction of separation but had separation regions up and downstream of the injection tubes. Tangential blowing proves the most effective in reducing separation to a minimum (Figs B-19, B-20). The optimal injection rate was found to be 4.6 lb/min. The mass flow rate for the duct was 29 lb/min.

The water table study provided a "map" of flow in the pipe, pinpointing regions of separation. The regions shown in Fig 5 could now be the focus of attention in the gas flow model, Phase II study. Furthermore, both methods of separation

22

control showed promise on the water table which merited further study in the full-scale gas model. Armed with the information gleaned from the water table, Phase II was begun.

Phase II: Gas Flow Model Study

Introduction. The second phase of testing was a direct follow-on to the water table study. The full-scale gas flow model studied only two areas indicated by the water table, i.e., separation at both turns. Again, the mass flow rates used were those dictated by the limitations on the aircraft, i.e., 1 lb/min and 8 lbs/min. High pressure air supply with a stilling chamber was used because smooth, uniform air could be pumped through the pipe, thus the inlet modification was not studied.

Apparatus. A full-scale light pipe was fabricated out of plexiglass. Figure 9 shows the experimental setup. The dimensions were the same as the actual light shown in Fig 3. A smoke injection system was used to visualize the flow field. The smoke was produced by a Cloud Maker Model No. 11-48, made by Testing Machine, Inc. The machine heated heavy mineral oil and dispersed it with compressed carbon dioxide. Because of the low velocities involved, measurements were made with an Alnor Series 6000-P Velometer manufactured by the Alnor Instrument Co. The scale on the instrument was in feet per minute and operated on a pitot-static system.

Photography was accomplished using a strobe lamp attachment to a Graflex camera loaded with 3000 speed Polaroid black

SECTION B-B

SECTION A-A
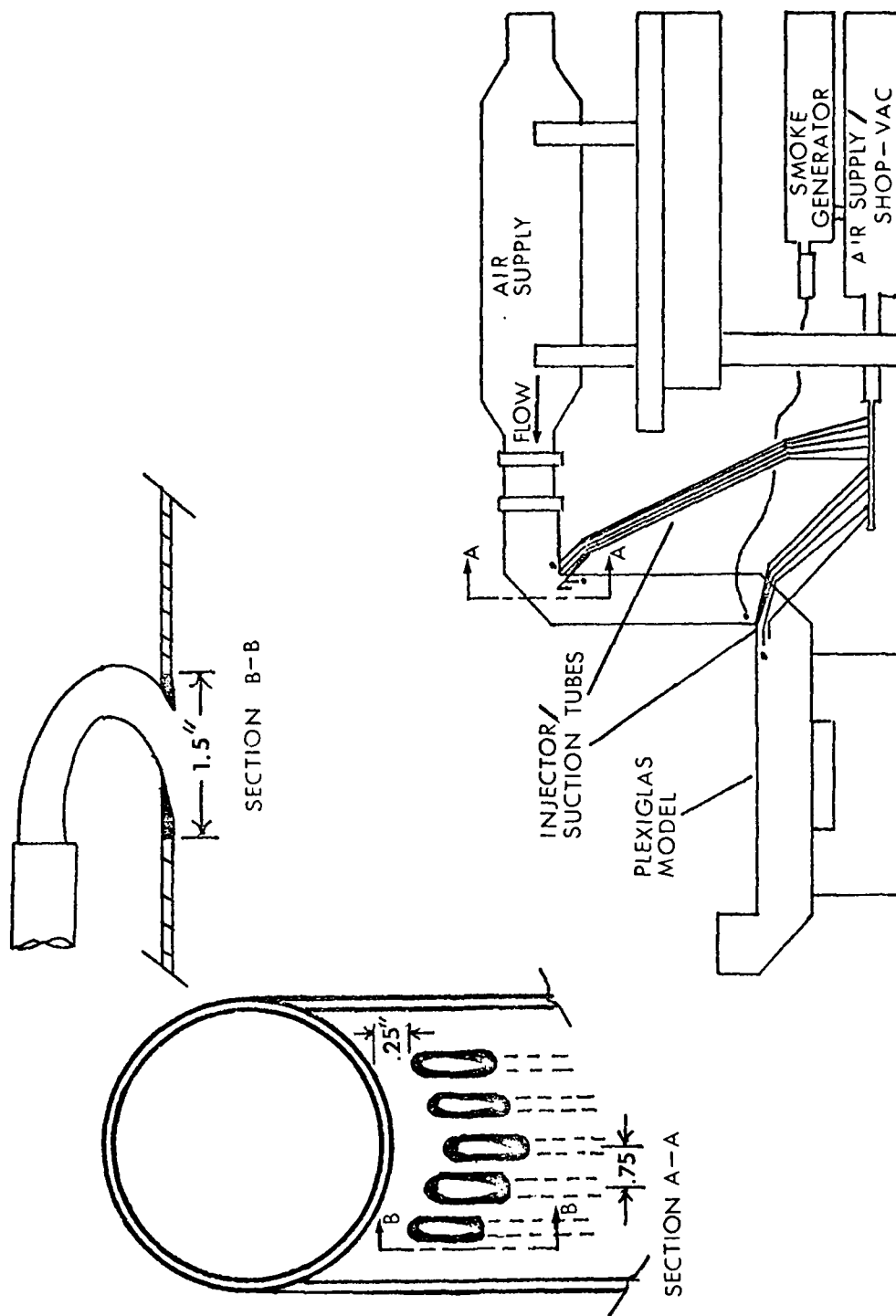
Fig 9. Gas Flow Model Experimental Setup With Injector/Suction Slots

24

and white film. The camera aperture was set at f.32 and had a shutter speed of four-hundredths of a second.

Procedure. Before the light pipe model was mounted, the desired mass flow rate was established. In order to do this, the Alnor Velometer was placed at the face of the laboratory high pressure air supply stilling chamber. A velocity of either 60 ft/min (1 ft/sec) or 780 ft/min (13 ft/sec) was set for each run. The light pipe model was then mounted to the air supply.

Smoke was injected into the model using a 0.12 inch diameter, L-shaped copper tube. The velocity of the smoke was measured using the Velometer to insure that the injection velocities did not exceed the freestream velocities, but rather matched them. With the CO_2 pressure gauge set at 10 psi, injection velocities of 1 ft/sec were attained. The injection system maximized injection velocities at 20 psi, making the injection velocities for high freestream velocities less than freestream. The smoke injection was done by the L-shaped tube to produce tangential injection in the same direction as the freestream. Smoke injection was accomplished at the first and second turns, above and below each. Figure 9 indicates injection positions by a small dot on the pipe. The smoke injector was used at only one position at a time. Since the smoke ran continuously, the injector was activated and the particular flow separation control was studied.

Smoke was injected at both positions downstream of each corner and shut off instantly. The time it took for the smoke

25

to dissipate completely from the separated regions was measured, i.e., mass turnover times. This measurement would aid in determining radial temperature gradients in the pipe since absorption is time dependent. This was done for both flow rates, 1 lb/min and 8 lbs/min.

A detailed study of both corners was made using smoke injection and photographing the resulting visible flow field. Photographs were made without smoke injection to serve as a reference for those taken with smoke. Again, both flow rates were scrutinized. The study included research into the effect separation control at one elbow would have on the other elbows. The complete set of data referenced in the results section that follows is in Appendix C.

Results. As seen in Figs C-1 to C-4, the separated regions associated with the first and second turn are as large as those predicted by the water table study. Figures C-1C and C-2B illustrate that the flow is indeed turbulent.

The light pipe model was modified to provide mass injection at both corners. Figure 9 shows the positioning of the injectors. Slots were devised as a method of injecting air as closely to the wall as any configuration while still keeping the physical constraints of the problem in mind (see section A-A Fig 9). Curved tubing allowed the air to change direction and enter the pipe close to the wall. High pressure laboratory air was used for the injection. Separate valving from this air supply allowed the two injection systems to be operated independently. As smoke was being injected into the tube, the

26

mass injection systems were operated to determine the effect on reducing the separation regions. Figures C-5, -6, and -7 show the effectiveness of blowing. For V = 13 ft/sec, Fig C-5C shows the separation seen in Fig C-5B reduced by blowing. Likewise, for V = 1 ft/sec, Figs C-6B to C-6D shows the separation decreasing as blowing is increased. The amount of remaining separation can be seen in Fig C-7B.

Blowing at the first turn did have adverse effects downstream. As mass was being injected at the first turn, the side opposite the injectors just upstream of the second turn experienced flow reversal. Flow reversal occurred at the slightest introduction of blowing upstream. Figures C-8 and -9 show flow reversal and its progressing severity as blowing was increased. Blowing at the second turn had little effect on alleviating the reversal.

The model was then used to determine the effect suction would have on separation. The model configuration remained unchanged. The injector tubes were connected to a vacuum cleaner (Shop-Vac) to provide the suction, which was not capable of varying the 8 lbs/min suction rate available at the hose connection orifice. Each corner had its own Shop-Vac. Again, smoke was injected to determine the effect suction had on the flow field. In this instance, only the lower flow rate was studied since a high enough suction could not be created to affect the higher flow rate. Figures C-10 through C-13 contain photographs of the suction results. Figures C-10 and -12 show by comparison that the separation region is minimized

27

at both corners. Figures C-11 and -13 illustrate the continued motion of the flow downstream of the suction tubes. No adverse effect was noted by applying suction to both corners simultaneously. The suction system at each turn seemed to have no effect on the other.

It was found that the turnover time (time to clear the smoke from the recirculation zone) was 3.5 seconds for the 1 lb/min flow rate. The turnover time for the 8 lbs/min appeared to be instantaneous, however, based on the water table observations, the time can be estimated to be 0.1 second.

Having looked at the experiment in detail and reviewing the results, the overall results can now be analyzed along with their implications.

IV. Discussion of Overall Results

Water Table Results

The water table revealed three separated regions:
1) inlet; 2) turn #1; and 3) turn #2. Also, the flow was
turbulent at both mass flow rates. Modification to the model
to control and reduce separation was tried.

A bell mouth inlet modification to the water table
model alleviated the separated region just inside the inlet.
The incoming streamlines proved smoother.

Mass injection exhibited promise in separation control
when applied tangentially. Normal injection only aggravated
the separation. Angular injection of 45 deg reduced separation
but showed areas of separation just upstream of the injectors
and underneath the injection fluid. For the higher flow rate,
a mass injection of 4.63 lbs/min was required to reduce separa-
tion. The injection velocity was 3.3 ft/sec.

Suction removed the separation region more completely
than injection. The capacity of the suction system was ex-
ceeded at the higher flow rate of $V = 1$ ft/sec. The mass
removal rate was approximately 7 lbs/min.

Gas Flow Results

A comparison of the data collected on the water table
to that of the gas flow model show good agreement in size of
the separation regions. Fifty percent of the tube is under

29

the influence of separation after turning the first corner.
Figure 3 shows the dimensions and the observed shape of the
separated regions. From the photographs, the dimensions for
the separated regions at both corners and both flow rates were
found to be extending across 75 percent of the tube from the
wall radially across the tube. The length of the region was
found to be one tube diameter long along the wall. These are
maximum dimensions with the overall shape of the separated
region.

Mass injection was successful in removing the separated
region associated with both turns #1 and #2. The mass injec-
tion rate for both flow rates was .185 lb/min. Increasing
the injection rate did not effect the flow any further. There
was, however, an anomalous, undesired flow characteristic
associated with mass injection. The mass injection at turn
#1 caused the opposite side of the tube (away from the injec-
tors) to experience flow reversal beginning near turn #2.
The flow reversal, in essence, stagnated the complete outer
side of the tube. This area extended from the point opposite
the injectors to the corner of turn #2. This large separated
region was more severe than the normal separated regions
associated with the uncontrolled flow.

Suction utilizing the existing blowing slots was
successful in reducing the separated regions to a minimum of
about one-tenth of the tube diameter in size. Suction was
done with no adverse flow effects. Suction applied to one
corner and then the other had no noticeable effects on the

flow where suction was not applied. It was observed that by cutting off the suction supplied by the two outside tubes, the separation tube re-established itself. The higher flow rate of V = 13 ft/sec had no suction data taken because the vacuum systems available were not strong enough to affect the separation. A stronger vacuum would have been effective in reducing the high velocity flow separation.

Absorption Results

From the results gleaned in Phase II with the gas flow model with no separation control, a characteristic time of exposure (Δt) for the separated regions was found for both flow rates, i.e., Δt = 3.5 seconds for V = 1 ft/sec and Δt = 0.1 second for V = 13 ft/sec. The exposure times are considered worse cases and were applied to the absorption calculations. These transient times are considered to be enough to set up a thermal lens. The lens can be considered fully developed in the time it takes for an acoustic wave to traverse the laser beam radius which, in this case, is 2×10^{-4} sec (Ref 7:1692). The thermal lens is, of course, the result of molecular absorption. All of the calculations were based on the following beam and air characteristics:

laser wavelength (CO_2), λ = 10.6 μm
laser power, P = 1 megawatt
absorption coefficient, k = .1/km
beam radius, r = 5.67 cm
gas temperature, T = 70F
beam path length, L = 175.26 cm

The flow of 1 ft/sec resulted in temperature rises above the ambient in the separated regions of $\Delta T = 52$ F, while the 13 ft/sec flow experienced a rise of $\Delta T = 2$ F. Table I gives the results for both flow rates of the beam distortion. The OPD and δ were calculated by comparing beam path A and path B, shown in Fig 5. Notice that path B does not encounter separated regions. Path A was considered to traverse 28 cm of separated region, i.e. heated air, neglecting the inlet separation.

TABLE I

Beam Distortion Results

Flow Speed (fps)	$\Delta T(F)$	OPD(cm)	δ(waves)
1	52	6.4×10^{-4}	3.8
13	2	2.0×10^{-5}	0.1

With suction applied to each corner at V = 1 ft/sec, the pathlength the laser beam would traverse through the separated region was reduced to one-tenth of a beam diameter. The associated distortion was within the acceptable one-tenth wave distortion. The distortion related to the V = 13 ft/sec without separation control also fell into the acceptable level.

V. Conclusions

From experimental investigation of the flow field in
the light pipe, both on the water table and the gas flow
model, conclusions can be drawn about the overall flow
character. Separation region sizes and mass turnover times
in these regions allowed estimations of molecular absorption
effects on the laser beam in the light pipe with and without
separation control. The conclusions drawn from the theoreti-
cal calculations and experimental results are listed below.

1) The axisymmetric water table simulation was an
accurate method for simulation of the 3-D pipe flow model.

2) The flow in the ALL APT light pipe is fully turbu-
lent, which provides excellent mechanical mixing, resulting
in thermal equilibrium in the pipe main flow.

3) Mass injection is not an alternative in removing
the separated regions in the light pipe due to severe flow
reversal.

4) Suction is a method capable of removing separation
regions at the low flow rate, i.e. $\dot{m} \simeq 1$ lb/min, in the
light pipe and reducing the beam degradation across the beam
by 97 percent.

5) Increasing the mass flow rate through the light
pipe will reduce the beam distortion due to absorption in the
separated regions. The reduction can be as much as 97 percent

of the phase distortion at 1 lb/min by using 8 lb/min flow rate.

6) Flow separation control is required at 1 lb/min to alleviate beam degradation.

VI.   Recommendations

Based on conclusions from both experiment and calculation, the following recommendations can be made:

1)   For the present configuration, suction is a method that should be applied to the ALL APT light pipe to reduce absorption.   This method does not introduce a different temperature gas as would mass injection.   Suction should be applied for the lower flow rates.   As flow rates increase, the need for separation control is diminished.   There are obvious gray areas where the flow rate may not remove the heat fast enough.   Therefore, it is suggested that further study be applied to determining maximum suction rates the flow can tolerate as well as absorption toleration levels.   The suction configuration tested is totally compatible with the actual ALL APT light pipe.   The suction configuration is not optimized, and if further study is contemplated, it should be done in optimizing this configuration.

2)   It is recommended that any future light pipes have curved elbows.   By doing this, adverse pressure gradients can be avoided and, thus, do away with separation.   A water table study was done to illustrate the effectiveness that this simple geometrical change can have on the flow characteristics.   Based on previous work done on elbows in heating ducts (Ref 11), the water table model was modified to have an inside elbow radius

of 4 inches. The dramatic results can be seen in Figs 10 and 11, which are for the high and low speed cases, respectively. The flow is now free of stagnation regions. This was true for both the high and low speed cases.

Figure 40. Modified Elbow at Turn #2, Outside Radius of 4 Inches, V = 1 ft/sec.

Figure 11. Modified Elbow at Turn #2, Outside Radius of
4 Inches, V = 0.1 ft/sec.

38

Bibliography

1. Schlicting, H. Boundary Layer Theory. New York: McGraw-Hill Book Company, 1968.

2. Johnson, J.P. "Internal Flows," Topics in Applied Physics: Turbulence, Volume 12, edited by Peter Bradshaw. Heidelberg and New York: Springer-Verlag, 1978.

3. Duffie, J.A. and W.A. Beckman. Solar Energy Thermal Process. New York: John Wiley & Sons, Inc., 1974.

4. Roach, W.T. "The Absorption of Solar Radiation by Water Vapour and Carbon Dioxide in a Cloudless Atmosphere," Quarterly Journal of the Royal Meteorological Society, 87: 364-373 (July 1961).

5. Hottel, H.C. "Radian-Heat Transmission," Heat Transmission, edited by William H. McAdams. New York: McGraw-Hill Book Company, Inc., 1954.

6. McClatchey, R.A. and J.E.A. Selby. Atmospheric Transmittance, 7-30 μm: Attenuation of CO_2 Laser Radiation. AFCRL-72-0611. L.G. Hanscom Field, MA: Air Force Cambridge Research Laboratories, October 1972.

7. Smith, David C. "High-Power Laser Propagation: Thermal Blooming," Proceedings of the IEEE, 65: 1679-1714 (December 1977).

8. Valley, George C., et al. "Thermal Blooming in Axial Pipe Flow," Applied Optics, 18: 2728-2730 (August 1979).

9. Kreith, Frank. Principles of Heat Transfer. Scranton: International Textbook Company, 1969.

10. Meyer-Arendt, Jurgen R. Introduction to Classical and Modern Optics. Englewood Cliffs, NJ: Prentice-Hall, Inc., 1972.

11. Wirt, Loring. "New Data for the Design of Elbows in Duct Systems," General Electric Review, 30: 286-296 (June 1927).

12. Pope, Alan and John J. Harper. Low-Speed Wind Tunnel Testing. New York: John Wiley & Sons, Inc., 1966.

13. Harleman, R.F. and Arthur Ippen. Studies on the Validity of the Hydraulic Analogy to Supersonic Flow. U.S. Air Force Technical Report No. 5985, January 1950.

14. Orlin, W.J., et al. "Application of the Analogy Between Water Flow with a Free Surface and Two Dimensional Compressible Gas Flow." NACA TN 1185, February 1947.

15. Giles, Ronald V. Schaum's Outline of Theory and Problems of Fluid Mechanics and Hydraulics. New York: McGraw-Hill Book Company, 1962.

APPENDIX A

Hydraulic Analogy

In order to determine the equations that apply in the
hydraulic analogy, the exact properties of the fluid to be
simulated must be found. The gas flow to be simulated is
air flowing through a 5.25 inch diameter pipe at an altitude
of 5000 ft at mass flow rates that range from 1 lb/min to
8 lbs/min.

From these parameters, the corresponding velocities of
the flow can be determined from

$$\dot{m} = \rho A V \qquad\qquad (A-1)$$

The resulting velocity range for the corresponding mass flow
rates is 1.68 ft/sec (1.15 mph) to 13.45 ft/sec (9.17 mph).
From the velocity, the Mach number can be calculated from

$$M = V/a \qquad\qquad (A-2)$$

Hence, the Mach number ranges from $M = 0.001$ to $M = 0.01$.

According to Pope and Harper, the flow can be considered
incompressible below 300 mph (Ref 12:1), which is well within
the speed range being considered. The assumption can also
be made that at such low velocities the flow is adiabatic;
that is, no heat is transferred to the fluid by its surroundings
and vice versa.

The basic equations governing fluid flow apply to both water and air. The major discrepancy arises in the specific heat ratios of the two fluids. For water, the specific heat ratio is 2, whereas for air it is 1.4. This discrepancy can be neglected, however, since the flow is assumed adiabatic (Ref 13: Part II, 3). This assumption may affect discrete quantities in the flow field, but not the overall quality of the flow (Ref 14:9). The hydraulic analogy can be summarized as follows (Ref 14:7):

AIR	WATER
Temp ratio, T/T_o	Water-depth ratio, d/d_o
Density ratio, ρ/ρ_o	Water-depth ratio, d/d_o
Pressure ratio, P/P_o	Square of water-depth ratio, $(d/d_o)^2$
Velocity of sound, a	Wave velocity, $\sqrt{gd}$
Mach number, M	Mach number, $V/\sqrt{gd}$

Of these parameters, the combination of these in.o non-dimensionalized force ratios provides the key to similitude in fluid flows (Ref 12:3). The following three non-dimensional are the basis for similarity:

$$\text{Reynolds number (Re)} = \frac{\text{Inertia Force}}{\text{Viscous Force}}$$

$$\text{Mach number (M)} = \frac{\text{Inertia Force}}{\text{Elastic Force}}$$

$$\text{Frounde number (Fr)} = \frac{\text{Inertia Force}}{\text{Gravity Force}}$$

Below M = 0.4, the Mach number loses its significance (Ref 12:3), which is the case at hand since the flow is at maximum M = 0.01. Since this study concerns flow in a pipe

42

and pipe flows are subject primarily to *viscous* and *inertia* forces when considered in a horizontal plane, then the only parameter necessary is Reynolds number. Because the flow is horizontal, the Frounde can be neglected, i.e., no gravity forces (Ref 15:63). Therefore, for the light pipe, the hydraulic analogy is based solely on equating Reynolds numbers. Then

$$Re_{air} = Re_{water}$$

or

$$\frac{Vd}{\nu}\Big|_{air} = \frac{Vd}{\nu}\Big|_{water}$$

The velocities in air and water from the above considerations become

$\dot{m}$ (lb/min)	Air (ft/sec)	Water (ft/sec)
8	13.45	1.68
1	1.023	0.12

APPENDIX B

Water Table Data

This data section contains the most representative photographs of the water table experiment. Reference to Fig 5 of the main text is contained in the figure captions. In all cases, the pictures are oriented such that the water flow is from the top of the photo to the bottom of the photo.

Figure B-1. Inlet, V = 1 ft/sec. a) No Dye Injection; b, c & d) With Dye Injection.

Figure E-2. Inlet, V = 1 ft/sec. All With Dye Injection.

Figure 1-5. Inlet, V = 1 ft/sec. All with ... diverters.

47

Figure E-1. Inlet, V = 0.1 ft/sec. a) No Dye Injection.
b, c & d) With Dye Injection.

48

Figure F-5. Channel Between Inlet and First Turn,
V = 1 ft/sec. a) No Dye Injection, b & c)
Dye Injection
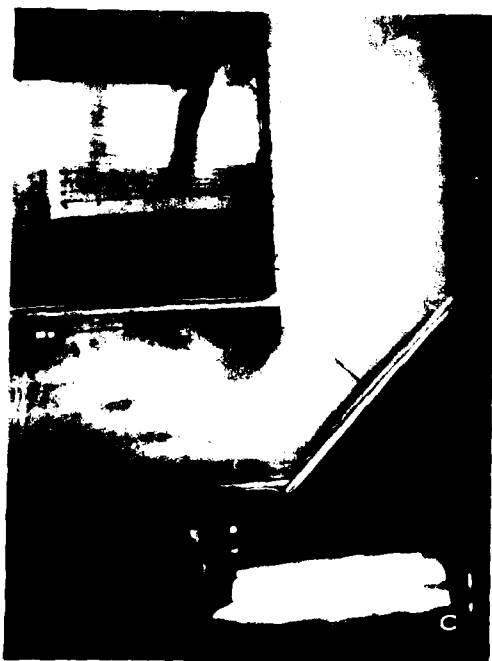
Figure B-6. Turn #2, V = 1 ft/sec. All With Dye Injection.

50
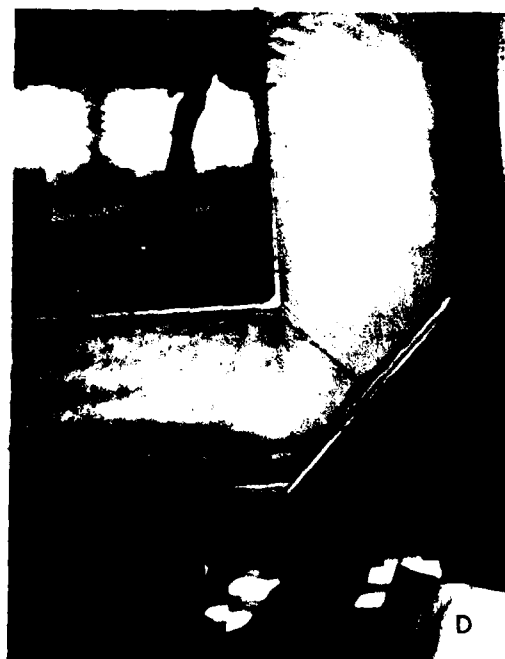
Figure B-7. Turn #2, V = 1 ft/sec. All With Dye Injection.

51
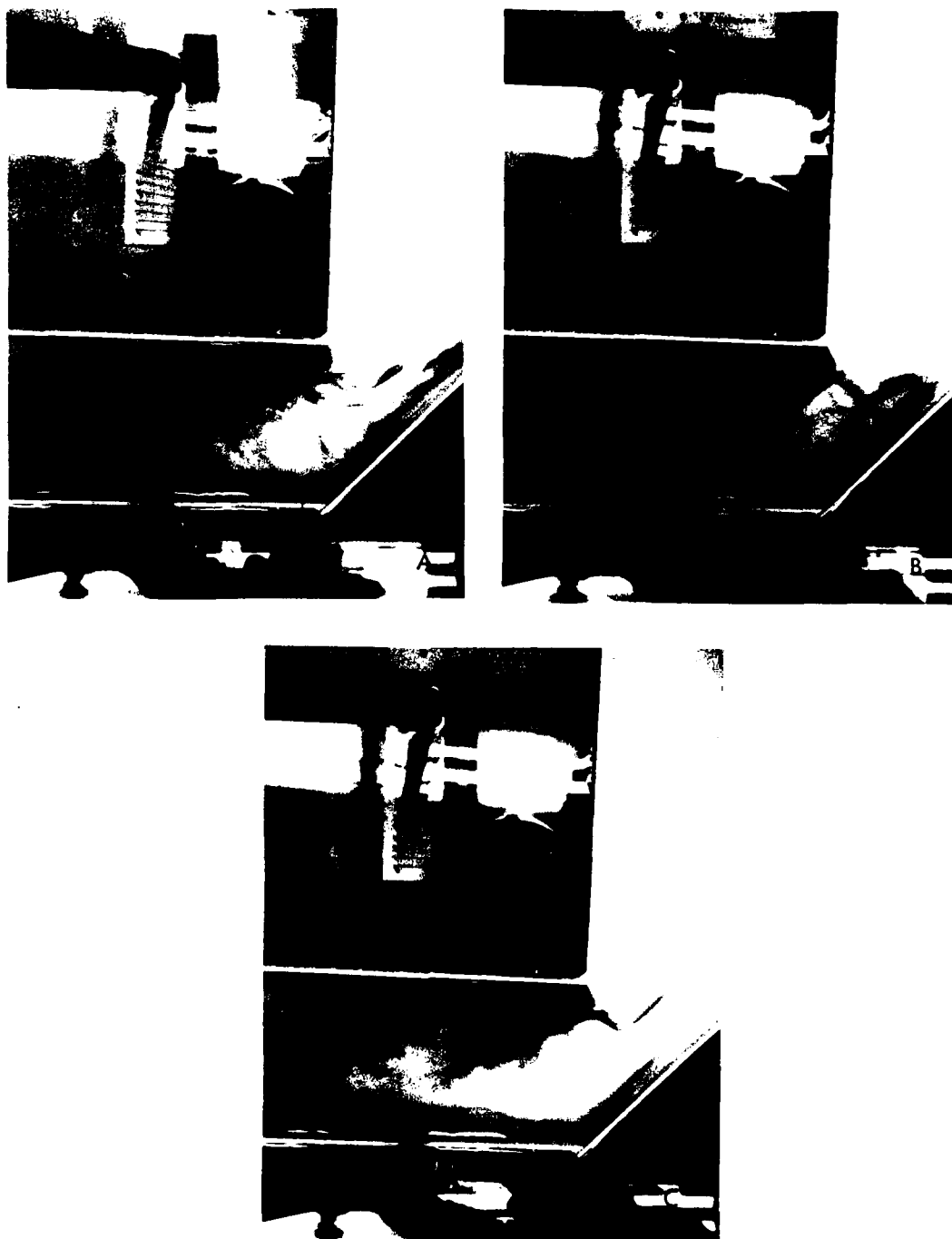
Figure B-8. Turn #2, V = 0.1 ft/sec. All With Dye Injection.

Figure B-9. Exit. a) No Dye Injection, V = 1 ft/sec.
b & c) Dye Injection, V = 1 ft/sec; d) Dye
Injection, V = 0.1 ft/sec. (Flow left to
right)
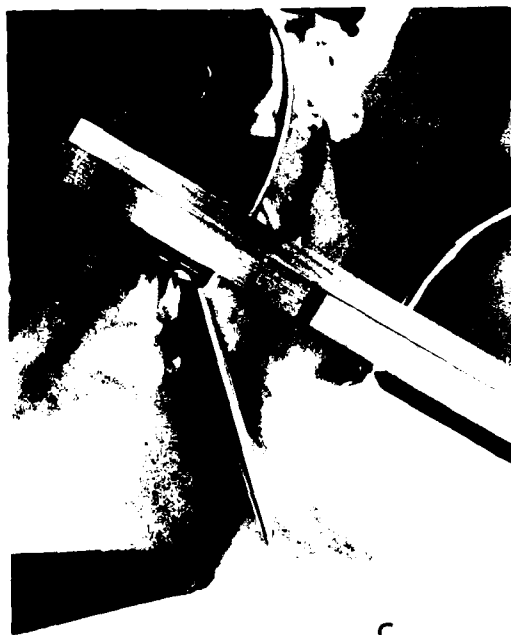
Figure B-10. Modified Inlet, V = 1 ft/sec. a) No Dye
Injection; b, c & d) With Dye Injection.

Figure B-11. Modified Inlet, V = 1 ft/sec. All With Dye Injection.

Figure B-12. Modified Inlet, V = 0.1 ft/sec. a) No Dye
Injection; b, c & d) With Dye Injection.

Figure B-13. Modification Effects, V = 1 ft/sec. a & b)
Turn #2 With Modified Inlet and Dye Injection; c & d)
Exit With Modified Inlet and Dye Injection (flow
left to right).

57

Figure E-11. Suction, Turn #2, V = 1 ft/sec. a & b) No Suction With Dye Injection; c & d) Suction With Dye Injection.

Figure B-15. Suction, Turn #2, V = 0.1 ft/sec. a & b)
No Suction With Dye Injection; c & d) Suction With
Dye Injection.

Figure B-16. Mass Injection, Normal, Turn #2, V = 1 ft/sec.
a) No Dye Injection; b & c) Mass Injection Normal
to the Flow With Dye Injection.

60

Figure B-17. Mass Injection, 45°, Turn #2, V = 1 ft/sec.
a & b) Dye Injection, No Mass Injection; c & d)
Mass Injection 45° Downstream with Dye Injection.
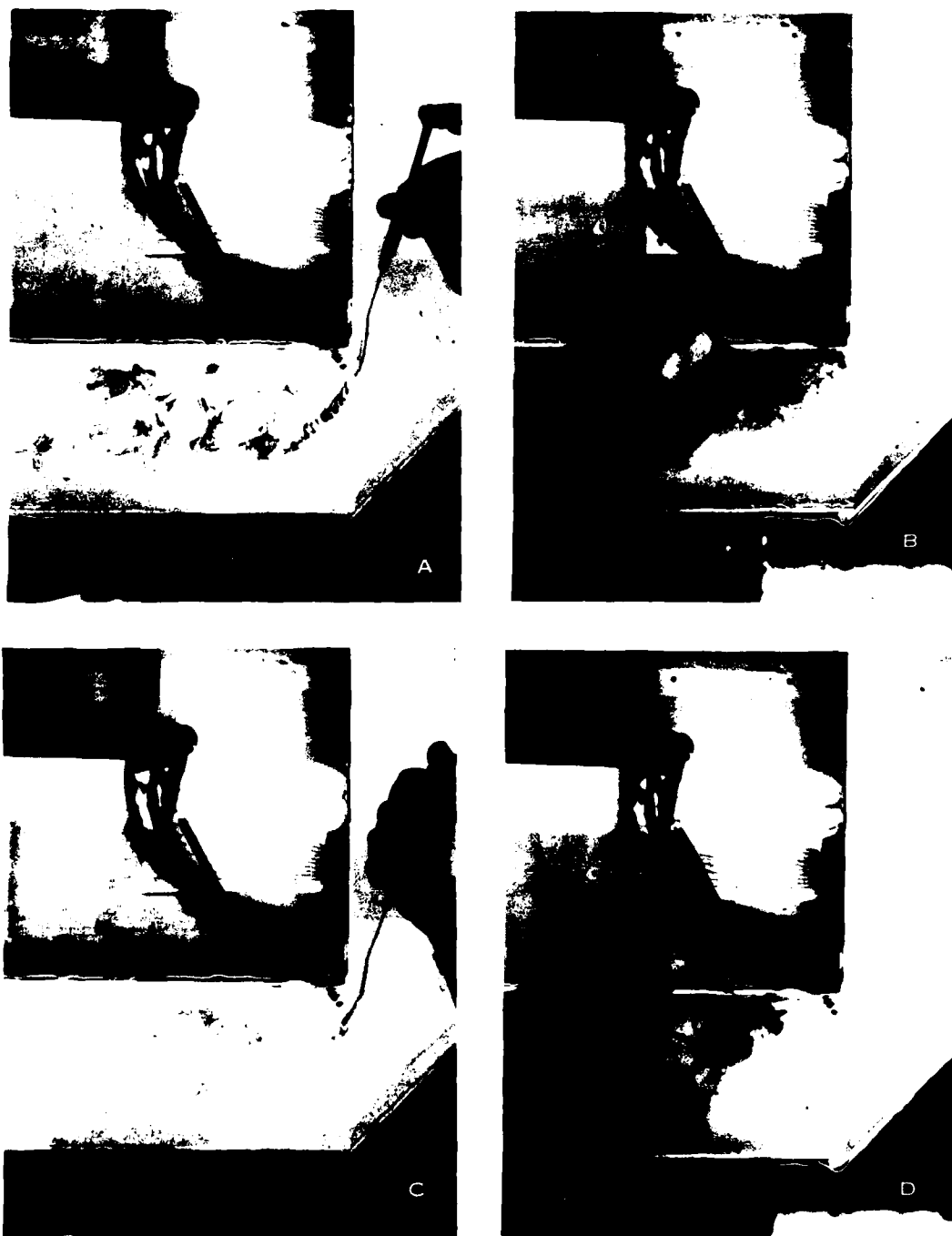
Figure B-18. Mass Injection, 45°, Turn #2, V = 0.1 ft/sec.
a & b) Dye Injection Without Mass Injection; c & d)
Dye Injection With Mass Injection 45° Downstream.

62
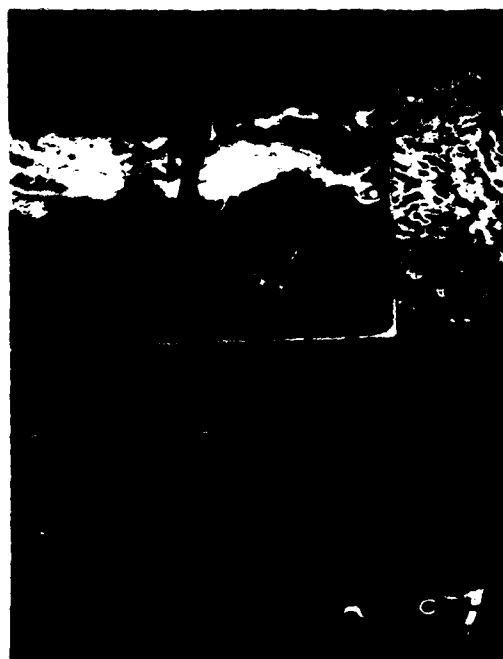
Figure B-19.   Mass Injection, Tangential, Turn #2,
V = 1 ft/sec.   a & b) Dye Injection Without Mass
Injection; c & d) Dye Injection With Mass Injection
Tangential to the Flow.

Figure B-20. Mass Injection, Tangential, Turn #2,
V = 0.1 ft/sec. a & b) Dye Injection With Mass
Injection Tangential to the Flow.

APPENDIX C

Gas Flow Data

The data collected from the gas flow model are contained in this appendix. In all cases, the air is blowing from top to bottom of page. For clarity, reference photographs without smoke have been included to aid in comparison.

Figure C-1.   Inlet, V = 13 ft/sec.   a) No Smoke Injection
b) Smoke Injection Downstream of Turn; c & d) Smoke
Injection Upstream of Turn.

Figure C-2. Inlet, V = 1 ft/sec. a & b) Smoke Injected
Upstream of Turn; c & d) Smoke Injected Downstream
of Turn.

Figure C-5. Turn #2, V = 13 ft/sec. a & b) Smoke Inject
Upstream of Turn; c & d) Smoke Injected Downstream
of Turn.

68

Figure C-4. Turn #2, $V = 1$ ft/sec. a) No Smoke Injection
b) Smoke Injected Downstream of Turn; c & d) Smoke
Injected Upstream of Turn.

69

Figure C-5. Mass Injection, Inlet, V = 13 ft/sec. a) No
Smoke Injection; b) Smoke Injection Without Mass
Injection; c) Smoke Injection With Mass Injection
(Smoke Injected Upstream of Turn)

Figure 6. Mass Injection, Inlet, V = 1 ft/sec.
a) Smoke Injection; b) Smoke Injection Without Mass
Injection; c) Smoke Injection With Nominal Mass
Injection; d) Smoke Injection With Full Mass
Injection (Smoke Injected Upstream of Inlet).

71
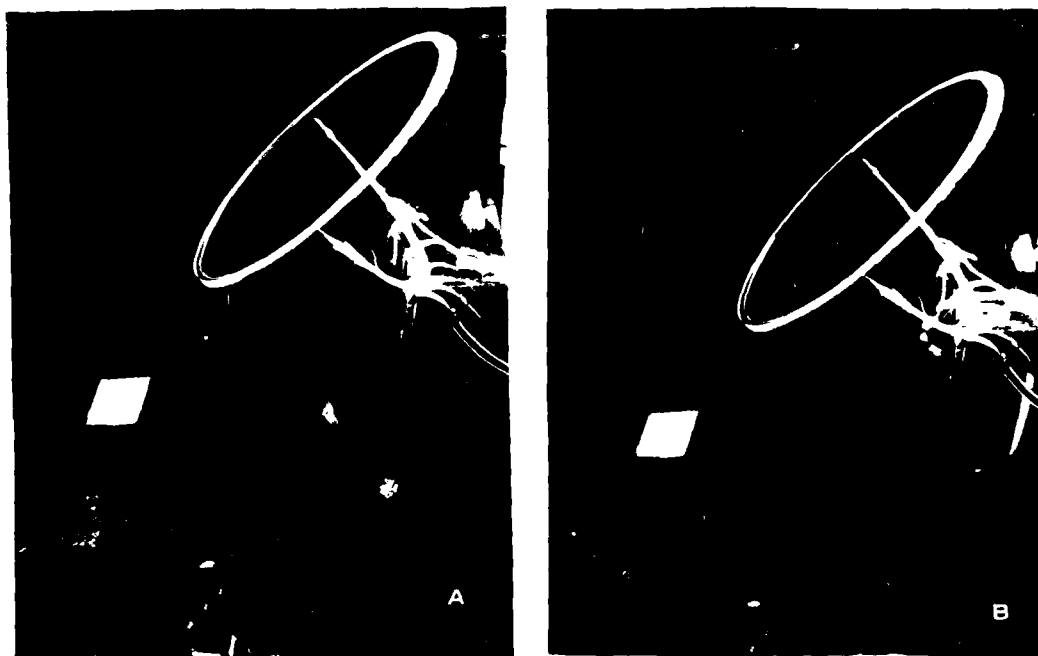
Figure C-7. Mass Injection, Inlet, ...
Injector located Upstream of ... ...
Injection; b) ... Injection ... ...
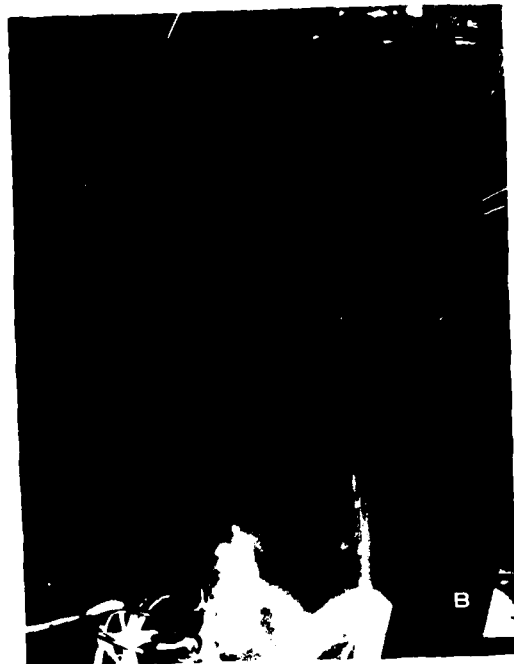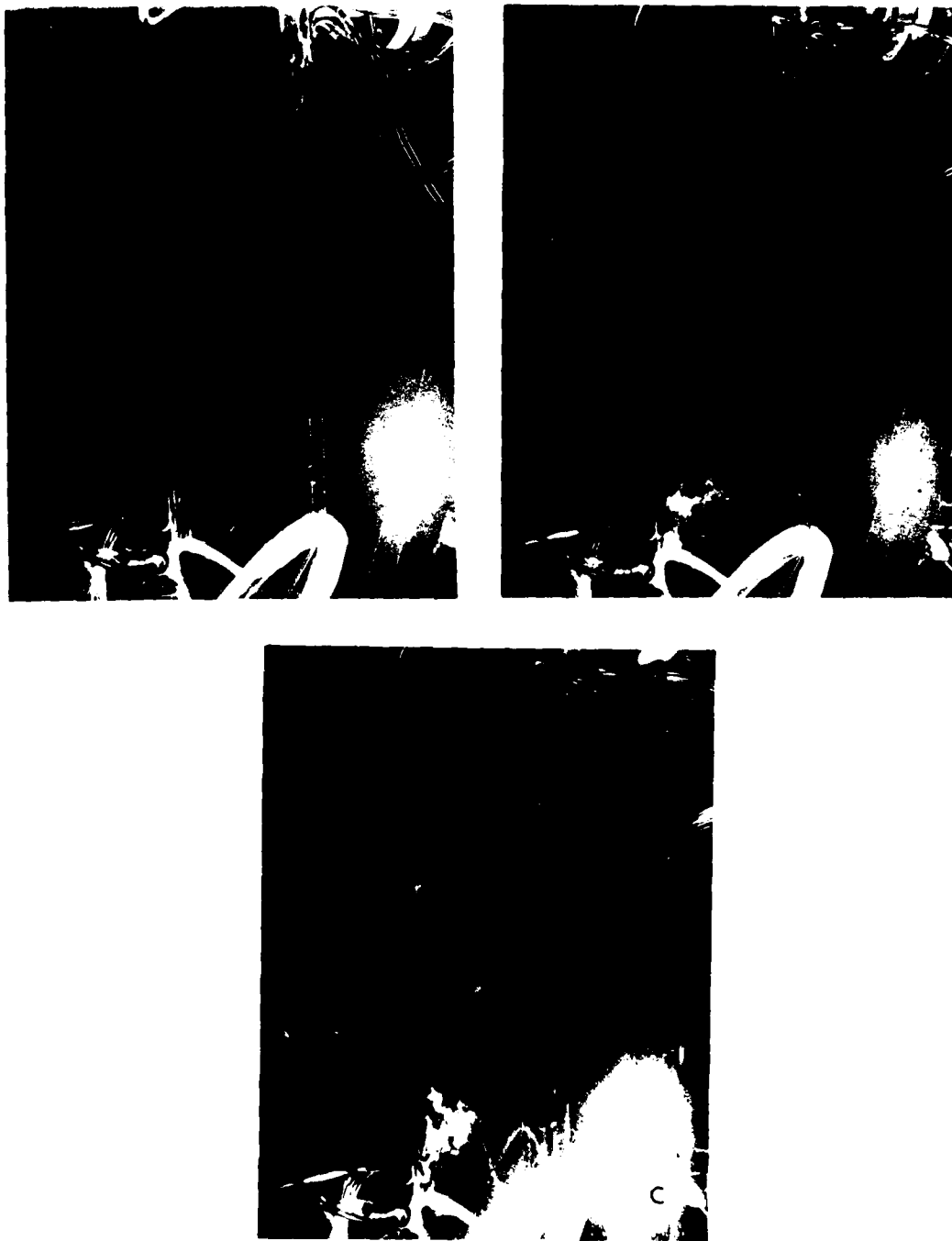
Figure C-9. Mass Injection Flow Reversal, Turn #2.
V = 1 ft/sec. a) No Smoke Injection; b) Nominal
Mass Injection at Inlet With Smoke Injected Upstream
of Turn #2; c) Maximum Mass Injection With Smoke
Injection Upstream of Turn #2.

74

Figure C-10. Suction, Inlet, V = 1 ft/sec. a) No Smoke
Injection; b) No Suction With Smoke Injected
Upstream of Turn; c & d) Suction With Smoke
Injected Upstream of Turn.

Figure C-11.   Suction, Inlet, V = 1 ft/sec., Smoke Injected
Downstream of Turn.   a & b) Without Suction;
c & d) Suction.

Figure C-12. Suction, Turn #2, V = 1 ft/sec., Smoke
Injection Upstream of Turn; a) No Smoke; b)
Smoke Without Suction; c & d) Smoke With Suction.

77

Figure C-15. Suction, Turn #2, V = 1 ft/sec., Smoke
Injection Downstream of Turn. a & b) Smoke
Without Suction; c & d) Smoke With Suction.

Vita

Wade H. Bailey, Jr. was born on 5 May 1948 in Beckley, West Virginia. He graduated from Woodrow Wilson High School in 1966 and attended West Virginia University, where he received the degree of Bachelor of Science in Aerospace Engineering. Upon graduation, he received a commission in the USAF through the ROTC program. He went directly to his initial assignment at the Foreign Technology Division at Wright-Patterson AFB as a telemetry analyst. His next assignment was to the Air Force Weapon Laboratory, Kirtland AFB, where he was engaged in measuring the atmospheric effect on laser beam propagation. The AFIT assignment followed the AFWL tour.

Permanent Address: 600 So. Oakwood Ave.
Beckley, W.Va. 25801

REPORT DOCUMENTATION PAGE		READ INSTRUCTIONS BEFORE COMPLETING FORM
1. REPORT NUMBER AFIT/GAE/AE/79D-1	2. GOVT ACCESSION NO.	3. RECIPIENT'S CATALOG NUMBER
4. TITLE *(and Subtitle)* SEPARATION CONTROL IN THE ALL APT LIGHT PIPE		5. TYPE OF REPORT & PERIOD COVERED Master's Thesis
		6. PERFORMING ORG. REPORT NUMBER
7. AUTHOR(*s*) Wade H. Bailey Jr. Captain USAF		8. CONTRACT OR GRANT NUMBER(*s*)
9. PERFORMING ORGANIZATION NAME AND ADDRESS Air Force Institute of Technology (AFIT/EN) Wright-Patterson AFB, OH 45433		10. PROGRAM ELEMENT, PROJECT, TASK AREA & WORK UNIT NUMBERS
11. CONTROLLING OFFICE NAME AND ADDRESS Air Force Institute of Technology (AFIT/EN) Wright-Patterson AFB, OH 45433		12. REPORT DATE December 1979
		13. NUMBER OF PAGES 90
14. MONITORING AGENCY NAME & ADDRESS*(if different from Controlling Office)* Air Force Weapons Laboratory (AFWL/LRO) Kirtland AFB, NM 87117		15. SECURITY CLASS. *(of this report)* UNCLASSIFIED
		15a. DECLASSIFICATION/DOWNGRADING SCHEDULE

16. DISTRIBUTION STATEMENT *(of this Report)*

Approved for public release; distribution unlimited.

17. DISTRIBUTION STATEMENT *(of the abstract entered in Block 20, if different from Report)*

19. KEY WORDS *(Continue on reverse side if necessary and identify by block number)*

Water table   Laser beam degradation
Absorption
Laser optical train
Thermal blooming

20. ABSTRACT *(Continue on reverse side if necessary and identify by block number)*

An experiment was performed to determine separation regions inside a high energy laser (HEL) beam relay light pipe. The pipe is part of the beam relay system used in confunction with the CO_2 Gas Dynamic Laser (GDL) system under development by the Air Force Weapons Laboratory. It was found that the air flowing through the pipe separated at the elbows. This separation can cause uneven radial heating attributed to molecular absorption.

The self-induced thermal distortion of the beam can cause phase distortions degrading the beam. A study of separation control systems within the pipe was made.

A full-scale axisymmetric model was studied on the water table. Areas of separation were found by flow visualization using dye injection. A brief evaluation of suction and blowing to control separation showed both of these methods acceptable. Separated regions discovered at each elbow on the water table were the focus of study for a full-scale air flow plexiglass model. The turbulent flow in the pipe was studied using smoke injection to reveal air motion in the pipe. Mass flow rates of air through the pipe were 1 lb/min and 8 lbs/min. Suction and blowing were assessed as flow separation control methods.

Blowing high speed air downstream of the inside of each elbow proved unacceptable as the outside of the pipe experienced flow reversal. Suction downstream of each elbow using small slots removed the separated regions completely at $\dot{m} = 1$ lb/min. Calculations of absorption within each of the separation regions for the flow rates of 1 and 8 lbs/min were made. Absorption calculations showed further that the 1 lb/min flow had temperature rises of 51 F and an associated phase distortion of 3 waves at 10.6 μm. The 8 lbs/min flow rate experienced a 2 F temperature rise, yielding a distortion of 0.1 wave at 10.6 μm.

It is recommended that suction as a means of separation control be applied to low mass flow rates through the tube due to unacceptable distortions to the beam. At high mass flow rates through the pipe, suction may not be possible; however, the associated beam distortions may be acceptable.